Long-term earthquake clustering: A 50,000-year paleoseismic record in the Dead Sea Graben

Shmuel Marco,[1] Mordechai Stein, and Amotz Agnon

Institute of Earth Sciences, Hebrew University, Jerusalem, Israel

Hagai Ron

Institute for Petroleum Research and Geophysics, Holon, Israel

Abstract. The temporal distribution of earthquakes in the Dead Sea Graben is studied through a 50,000-year paleoseismic record recovered in laminated sediments of the Late Pleistocene Lake Lisan (paleo-Dead Sea). The Lisan represents more than 10 times the 4000 years of historical earthquake records. It is the longest and most complete paleoseismic record along the Dead Sea Transform and possibly the longest continuous record on Earth. It includes unique exposures of seismite beds (earthquake-induced structures) associated with slip events on syndepositional faults. The seismites are layers consisting of mixtures of fragmented and pulverized laminae. The places where the seismites abut syndepositional faults are interpreted as evidence for their formation at the sediment-water interface during slip events on these faults. Thicker sediment accumulation above the seismites in the downthrown blocks indicates that a seismite formed at the water-sediment interface on both sides of the fault scarps. Modern analogs and the association with surface ruptures suggest that each seismite formed during a $M_L \geq 5.5$ earthquake. The ^{230}Th-^{234}U ages of a columnar section, obtained by thermal ionization mass spectrometry, give a mean recurrence time of ~1600 years of $M_L \geq 5.5$ earthquakes in the Dead Sea Graben. The earthquakes cluster in ~10,000-year periods separated by quiet periods of similar length. This distribution implies that a long-term behavior of the Dead Sea Transform should be represented by a mean recurrence of at least 20,000 year record. This observation has ramifications for seismic hazard assessment based on shorter records.

Introduction

The knowledge of past long-term behavior of seismogenic faults is a key to understanding earthquake physics and related hazard assessment. Studies of paleoseismic records are often hindered by difficulties in identifying the correct earthquake indicators, finding a sufficiently large time window, obtaining continuous records, and dating the events either relatively or absolutely.

The mean recurrence period of strong earthquakes is significant because it is a measure of the strength of the fault and of the rate of stress buildup [*Scholz*, 1990]. However, it gives no information on the pattern of event distribution through time. It has long been realized that slip on faults is cyclic, but its detailed temporal distribution and the patterns of its periodicity are still unclear, partly because the instrumental and preinstrumental records are usually either incomplete or too short. In the cases of short records, earthquake clustering may cause a serious deviation in the estimated recurrence period. Clustering has been inferred where there is a marked contrast between seismic rates of the last several centuries and rates over thousands of years or longer [*Grant and Sieh*, 1994; *Swan*, 1988]. Clustering might bias

estimates of seismic efficiency (the ratio of seismic to geologic slip) that may provide information on the mechanical properties of the faults. *Garfunkel et al.* [1981] estimate the seismic slip rate in the Dead Sea Transform in historical times at 15-50% of the Pliocene-Pleistocene geologic slip rate. A 90-year instrumental record yields seismic efficiency as low as 7% in the Dead Sea Transform [*Salamon*, 1993].

We report a 50,000-year, continuous, dateable paleoseismic record in the Late Pleistocene lacustrine Lisan Formation on the Dead Sea shore [*Marco et al.*, 1994]. The Lisan represents a time span more than tenfold the 4000 years of historical earthquake record [*Ben-Menahem*, 1991]. It is the longest and most complete paleoseismic record along the Dead Sea Transform and possibly the longest known record on Earth. The record includes seismites, a term introduced by *Seilacher* [1969], and used here for earthquake-induced structures in sediments, as proposed by *Vittori et al.* [1991]. We document their stratigraphic position, estimate their recurrence time, and analyze the temporal distribution of strong earthquakes. The data presented here provide direct evidence for long-term clustering of strong earthquakes in the Dead Sea Graben.

The Lisan Formation

Sediments of Lake Lisan are exposed along a 220-km length of the Dead Sea Transform, from Lake Kinneret (Sea of Galilee) in the north to the Arava Valley in the south (Figure 1). The deposits of this lake, the Lisan Formation, unconformably

---
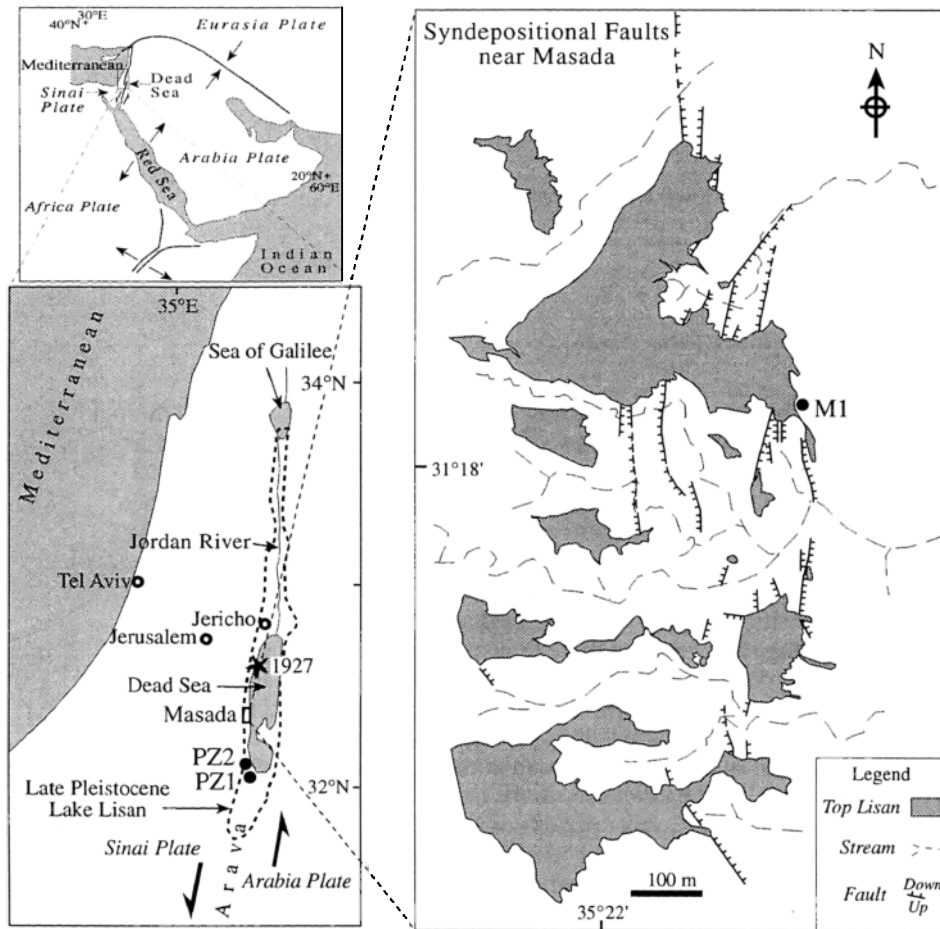
Figure 1. (right) The N-S striking fault zone near Masada includes syndepositional faults, which do not offset the top of the Lisan Formation. Solid circle marks the site of columnar section M1. (top) Plate tectonic setting of the Middle East. (bottom left) Sites of columnar sections PZ1 and PZ2 in the Peratzim Valley (solid circles); paleoshoreline of Lake Lisan (dashed). Star marks the epicenter of the 1927 earthquake [Shapira et al., 1992].

overlie earlier units. The Lisan Formation consists of alternating laminae of white aragonite and dark detritus. The white laminae are composed of aragonite; the detrital material contains fine-grained calcite, dolomite, aragonite, quartz, and clays [Begin et al., 1974]. Both types of laminae are up to a few millimeters thick. The paired laminae were interpreted as seasonal precipitates (varves): the aragonite is authigenic, possibly annual summer precipitate of Lake Lisan, whereas the dark laminae are detrital flood inputs into the lake during winter storms [Bentor and Vroman, 1960; Katz et al., 1977]. The extremely dry climate preserved the aragonite, which otherwise readily reacts with water and transforms to calcite [Katz and Kolodny, 1989]. The exceptional preservation of the varves that serve as sensitive stratigraphic markers, their similarity to the modern deposits of the Dead Sea, the continuous stratigraphic record, and the extensive outcrops along an active plate boundary (Figure 2), all make the Lisan Formation an ideal candidate for paleoseismic studies [El-Isa and Mustafa, 1986; Seilacher, 1984].

The Lisan sediments onlap all the canyons that flow to the Dead Sea and therefore postdate the period of the major landscaping. The ^{14}C dating and archeological artifacts [Copeland and Vita-Finzi, 1978; Neev and Emery, 1967; Vita-Finzi, 1964] indicate that the Lisan stage came to an end no earlier than 18 ka and perhaps somewhat later. U series dating

of aragonite from the Lisan Formation by α counting yielded ages of 71 to 18 ka with the stratigraphy [Kaufman, 1971; Kaufman et al., 1992]. The top 1.5-3.5 m of the Lisan Formation in the Dead Sea area is characterized by abundance

Figure 2. Typical view of Lisan Formation. The hard, gypsum-rich top of the formation forms a flat plain unaffected by syndepositional faults. Vertical exposures are about 40 m.

of gypsum and scarcity of aragonite. The above mentioned ages were all measured below this part of the section. Recently, thermal ionization mass spectrometry (TIMS) was applied to determine the U and Th isotopic compositions of aragonite samples from the Lisan Formation [Schramm et al., 1995; Stein et al., 1992]. U series dating by TIMS was successfully applied to aragonitic corals [Chen et al., 1986; Edwards et al., 1987]. Reproducible ages with uncertainty of less than 1% were obtained by TIMS for corals having very low concentrations of ^{232}Th and the ^{234}U/^{238}U activity ratios in equilibrium with seawater of 1.15±0.01 [Stein et al., 1993]. The advantage of the TIMS measurements over the conventional α counting is the significantly smaller sample that is required for analysis (facilitating the acquisition of highly pure aragonite samples) and the significantly higher precision in age determination . The problem with lake sediments, such as Lisan aragonite is twofold: (1) there is no apriori constraint on the U isotope composition of the water and (2) the amount of ^{232}Th is significantly higher than in coral aragonite; therefore "common" ^{238}U and ^{230}Th may be incorporated within the samples and, consequently, may affect the measured age. All these problems were thoroughly studied by A. Schramm et al. (manuscript in preparation, 1995). They found that pure aragonite samples (>99% aragonite) yield constant ^{234}U/^{238}U activity ratio of 1.50±0.02, which is indistinguishable from the value of present-day Dead Sea water [Schramm et al., 1995; Stein et al., 1992]. This result provides an important constraint for the assessment of ^{230}Th-^{234}U ages in the Lisan aragonite. The analytical error on pure aragonite Lisan samples (>99% aragonite) is less than 1%, yet the ages might be slightly too old due to presence of detrital ^{238}U, ^{234}U, and ^{230}Th associated with ^{232}Th.

The ages of section PZ1 (Figure 3) show that the lowest exposed layers are 71 ka old. Linear regression yields an average sedimentation rate of 0.86 mm/yr ($R=0.981$). A similar rate can be derived from the ages determined by Kaufman et al. [1992].
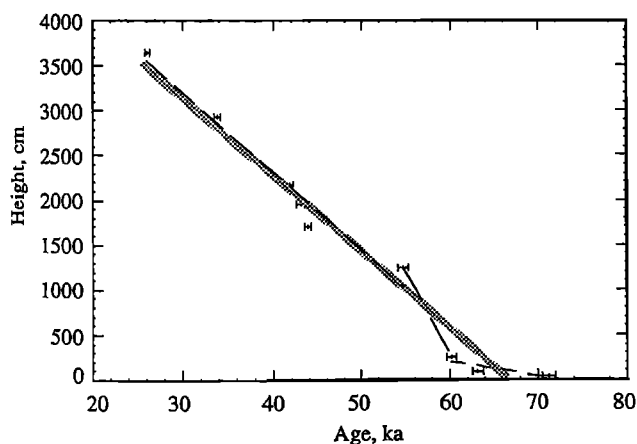
Figure 3. U series ages of nine horizons in section PZ1. Data are from Schramm et al. [1995] and A. Schramm et al. (manuscript in preparation, 1995). Error bars show 1% analytical uncertainty. Linear regressions of three segments (dashed) give sedimentation rates of 0.16 mm/yr in the lower 250 cm, 1.84 mm/yr from 250 cm to 1250 cm, and 0.88 mm/yr above 1250 cm. A single regression of the entire section (gray line) gives a mean sedimentation rate of 0.86 mm/yr.

The sediments in the study areas of the Peratzim Valley and Masada are characteristic horizontal lake bottomsets. Interfingering of varves and clastics in the range of sand to cobble conglomerate are common in alluvial fans at the margins of the graben valley, where they form typical foresets, in places overlain by topsets. The absence of intraformational erosion channels, hiatuses, or unconformities indicates that the deposition of the Lisan Formation bottomsets had been continuous. Fossil beach terraces at 180 m below sea level, paleontological considerations, and sediment chemistry led Begin et al. [1974] to conclude that the center of Lake Lisan was quite deep, reaching 200 m or even 600 m [Katz et al., 1977]. The lake level lowered rapidly at the end of a long period of dry climate.

The lowering of water level of the modern Dead Sea was accompanied by incision of canyons into the Lisan Formation, creating vertical exposures of more than 40 m.

Seismological Studies in the Region

Our current knowledge of the seismicity of the Dead Sea Transform is based on the following, mostly short-term records.

Current Seismicity

The Dead Sea Transform system produces most of the large earthquakes in the region (see the Seismological Bulletins of the Institute for Petroleum Research and Geophysics (IPRG) and Salamon [1993]). Microearthquakes ($1.0 \le M_L \le 5$) tend to concentrate near tensional features such as the Dead Sea Graben [Shapira and Feldman, 1987; van Eck and Hofstetter, 1990]. This observation is common to other large strike-slip faults [e.g., Lovell et al., 1987; Segall and Pollard, 1980]. Focal mechanisms of large events in the Dead Sea Transform generally show strike-slip or normal solutions [Salamon, 1993; van Eck and Hofstetter, 1990]. During the period 1919-1963 the frequency-magnitude relation, $\log N = a - bM$, where N is the average number of earthquakes per year with magnitude M [Gutenberg and Richter, 1954], from the Dead Sea to north of Lebanon, was such that $a=3.25$ and $b=0.8$ (Table 1). Different segments appear to have similar b values of 0.8 [Shapira and Feldman, 1987]. A compilation of seismicity for the last century yields a b value of 1 [Salamon, 1993]. Focal plane solutions of large events along the Dead Sea Transform confirm the plate tectonic model: the large events align with the trace of the transform and sinistral motion predominates. Microseismicity occurs over a broad area and shows a mixture of strike-slip and normal faulting [Ben-Menahem, 1991; Salamon, 1993; van Eck and Hofstetter, 1990]. The last destructive earthquake ($M_L=6.2$) struck the Dead Sea area in 1927. Its epicenter was about 25 km south of Jericho [Shapira et al., 1992].

Archeoseismicity

A compilation of 4000 years of historical seismological record [Ben-Menahem, 1991] infers that the mean return period of strong earthquakes along the 430-km-long Arava-Dead Sea-Jordan river segment was 1500 years. The estimated frequency-magnitude relation is $\log N = 3.10 - 0.86M$.

Paleoseismicity

El-Isa and Mustafa [1986] interpreted convolute folds in the Lisan as earthquake deformations in a previous study on the

Table 1. Frequency of Seismic Events From Previous Studies

Time Window	Frequency	Method	Reference
1927-1974	2/100 years of $M \geq 6$	instrumental	*Ben-Menahem et al.* [1976]
1919-1963	logN=3.25-0.8M	instrumental	*Arieh* [1967]
1733 y in Late Pleistocene	logN=5.24-0.68M	paleoseismicity	*El-Isa and Mustafa* [1986]
last 4000 years	logN=3.10-0.86M	historical reports	*Ben-Menahem* [1991]
last 2000 years	2/2000 years	trenches	*Reches and Hoexter* [1981]
50- 17 ka	1/1000-1/3000 years	trenches	*Amit et al.* [1994]
1900-1990	b=1	instrumental	*Salamon* [1993]
Late Pleistocene (?)-Recent	~thousands of years	seismic reflection	*Niemi and Ben-Avraham* [1994]

Lisan Formation on the east shores of the Dead Sea. El Isa and Mustafa concluded that during a period of 1733 years in the Late Pleistocene the average recurrence period was 340±20 years for $M_L \geq 6.5$, with a frequency-magnitude relation $logN=5.24-0.68M$.

In a trench study across the Jericho fault *Reches and Hoexter* [1981] identified two major earthquakes during the last 2000 years. Another trench study of Late Pleistocene alluvial fans in the southern Arava rift (about 180 km south of the Dead Sea) revealed multiple-event faults. *Amit et al.* [1994] and *Enzel et al.* [1994] estimate recurrence periods of 1000 to 3000 years for the period between 50 ka and 17 ka. *Gardosh et al.* [1990] estimate post-Lisan normal faults along the western shores of the Dead Sea to accommodate a subsidence rate of 0.85 mm/yr

Syndepositional Faults and "Mixed Layers"

Observations

Marco and Agnon [1995] discovered fault planes with vertical displacements up to 2 meters in the Lisan outcrop of the Masada area. Undisturbed layers that overlie the faults indicate that the faults are syndepositional. Deformed layers terminate at the faults (Figure 4). We call them "mixed layers" because they consist of mixtures of fragments of the two typical varve components of the Lisan Formation. In contrast to the common facies of laminated varves, the mixed layers exhibit unusual thickness, structure, and fabric. They are typically several centimeters to a few tens of centimeters thick (locally up to 1 m). They consist of nonlayered mixtures of fine-grained matrix and tabular fragments of varves of various sizes (several millimeters to centimeters). In places, fragment-supported texture shows a gradual upward transition to a matrix-supported texture (Figure 4). We used X ray diffraction to analyze the composition of three pairs of samples, taken from different localities. A pair consists of one sample of a mixed layer and one of its immediately underlying varves. The analyses show that the bulk composition of the varves varies between localities but the mixed layer composition is identical to that of underlying varves. No imbrication or other transport indicators were found. The mixed layers frequently overlie folded varve layers. These folds are asymmetrical and recumbent and in places exhibit box shapes. The typical wavelength is about 30 cm. The upper contact of the mixed layers is invariably sharp, but the lower contact is often irregular, intruded by fragments and mushroom-shaped diapirs from the underlying layers (Figure 5). Parts of the mixed layers exhibit sharp lower contacts. In several occurrences we found fissures that extend downward from mixed layers (Figure 6). These fissures are several centimeters wide, filled with material

from the mixed layer. No vertical displacement is observed across the fissures. Each mixed layer is restricted to a single stratigraphic horizon enclosed by undeformed beds. Mixed layers have been traced continuously over an area as large as the outcrop, i.e., hundreds of meters to a few kilometers.

Near the fault planes the mixed layers commonly contain cobble-sized laminated intraclasts that fell from the degrading scarp. The mixed layers are thicker in the downthrown block near the faults, filling 10-30 cm deep troughs. About 20-30 m away, the mixed layers thin out by a factor of 5 to 10 and maintain a uniform thickness throughout the outcrop area. Detailed sections across the syndepositional faults near Masada show thicker varve accumulation above the mixed layers in the downthrown block (Figure 4). The strike of the fault zone near Masada is parallel to the N-S trend of the Dead Sea Transform in the area (Figure 1). Strikes of individual fault planes are parallel to the strike of faults exposed in the main escarpment [*Agnon*, 1983]. The normal slip is consistent with the graben structure of the Dead Sea basin.

Interpretation

The mixed layers are interpreted as originally laminated layers that were fluidized, brecciated, partly resuspended, and then resettled. The crucial question is whether the mixed layers are seismites (earthquake deformations of the original varves) or they are produced by other processes, such as floods, storms, and slope failures.

Flash floods. Flash floods may trigger turbidity currents at lake bottom [e.g., *Hsü*, 1989]. However, the mixed layers are not turbidites because (1) they contain large varve fragments (Figure 4) which are extremely friable and would be expected to disintegrate completely during lateral transport in a turbulent flow, (2) the texture and fabric of each mixed layer are laterally uniform, which is an unlikely feature of turbidites, (3) in places the fragments at the bottom of the mixed layers can be restored to their original place, indicating little or no horizontal transport, and (4) no imbrication or other transport indicators are observed.

Evidence for flood events is exposed in incised alluvial fans near the outlets of canyons. These are wedges of coarse clastics in the range of sand to cobble conglomerate that interfinger with the lacustrine varves. The disturbances caused by these floods to the underlying varves do not extend beyond the coarse clastic intercalations. The mixed layers do not contain exotic clasts and are not associated with these wedges, which do not disturb the laminated bottomsets and do not form mixed layers. Recent floods spread out in the Dead Sea, forming a layer that floats above the dense lake water. The density of Lake Lisan was lower than the Dead Sea but higher
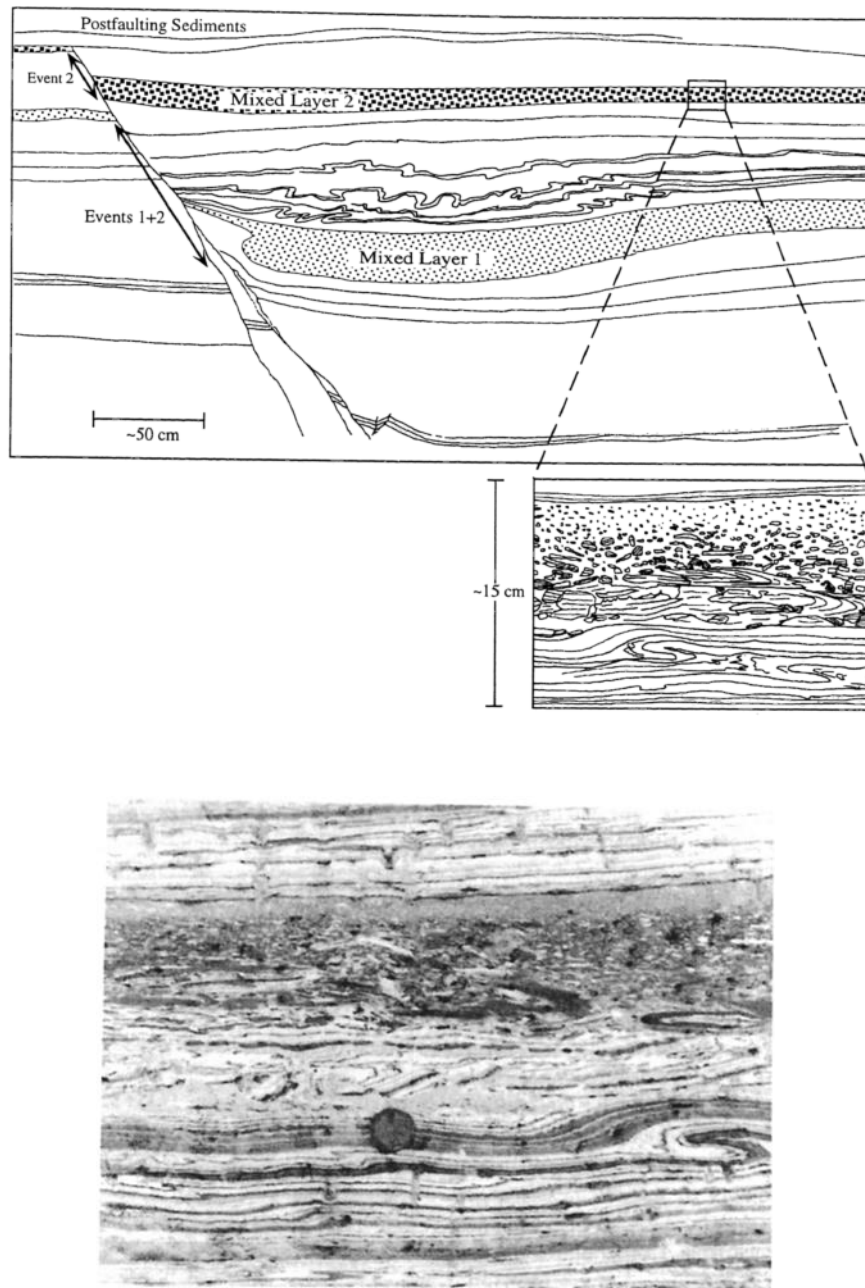
Figure 4. A syndepositional normal fault in the Lisan Formation near Masada unconformably overlain by undisturbed layers. Two mixed layers terminate at the fault in every block. They are thicker in the downthrown block, filling 10-30 cm deep troughs. The lower mixed layer in the downthrown block is also bent and overlain by folded varve layers that show local downdip transport. This folding formed by local slumping of varved layers into the trough. Lithologic markers show that the mixed layers correlate across the fault. They formed during two events when the fault slipped abruptly and ruptured the surface, creating a subaqueous scarp. Because of this scarp, sediment accumulation above the mixed layers in the downthrown block is thicker than in the footwall. A typical mixed layer (inset) shows a gradual upward transition from folded varves, through fragment-supported texture, to matrix-supported texture at the top. Such mixed layers are interpreted as earthquake deformations (partly traced from a photograph and partly drawn in the field). Photograph shows a mixed layer enclosed in a laminated sequence.

than seawater [*Katz et al.,* 1977] rendering flood-triggered turbidity currents impossible [*Hsü,* 1989].

Storm waves. By calculating the stress variation that is caused by the passage of surface waves one can estimate their effect at the bottom. Ten-meter-high storm waves with frequency of 0.1 Hz induce cyclic loading that is capable of triggering failure in low-strength sediments at a water depth that is comparable to the wave height [*Allen,* 1982]. Lake Lisan's highest water level was -180 m, and the depth of the center was at least 200 m [*Begin et al.,* 1974] and possibly 600 m [*Katz et al.,* 1977]. The studied outcrops are well below the depth affected by waves (except for the uppermost,
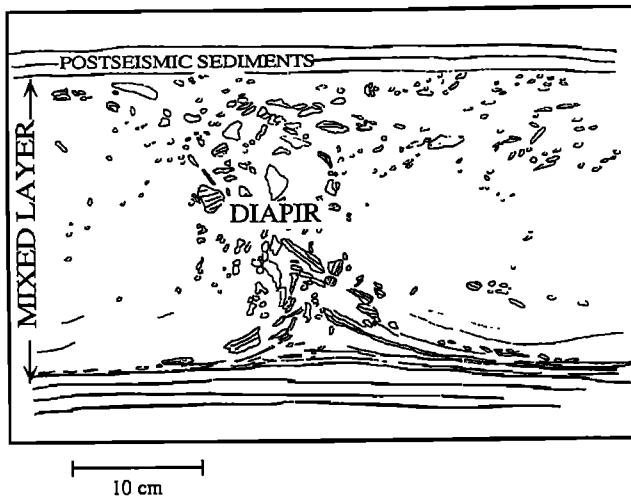
Figure 5. A trace of a photograph showing a diapir of varve fragments intruding the lower contact of a mixed layer. The intrusion must have occurred after the formation but before the consolidation of the mixed layer. It may have been triggered by an aftershock.

gypsum-rich layers, which were deposited as lake level was dropping). It is concluded that storms could not trigger the formation of mixed layers.

Slope failures. The considerations applied above to exclude turbidity currents and the horizontal position of the layers argue against gravity-triggered slope failure.

Seismically triggered sublacustrine slope failures accompanying historical earthquakes occurred mainly in alluvial fans and delta sediments, composed mostly of sand and gravel [Keefer, 1984]. The slope reported for these subaqueous landslides was at most localities steeper than 10° [Keefer, 1984], but an unusually low angle of 0.25° is reported in a single case [Field et al., 1982]. Seismic reflection profiles in the Dead Sea revealed slumped sediments in the Jordan River fan [Niemi and Ben-Avraham, 1994], showing the plausibility of earthquake-triggered slumps in other fans as well. The absence of alluvial fan components in the mixed layers, in addition to the preservation of the delicate varve fragments, indicates that turbulent mass flows from slope failures did not reach the flat bottom of the lake, where mixed layers formed.

Earthquakes. The conclusion of the discussion above is that flash floods, storm waves, and gravitational slope failures cannot explain the mixed layers. The following arguments point to earthquakes as the most plausible mechanism for the formation of mixed layers.

The mixed layers are flat-lying, restricted to single stratigraphic horizons. The extremely friable varve fragments and the absence of exotic components show negligible transport. Near Masada, the mixed layers abut syndepositional faults. The association of mixed layers with faults and with fissures filled by the mixed material point to their contemporaneous formation. Thicker varve accumulation above the mixed layers in the downthrown block (Figure 4) is indicative of a fault scarp that formed simultaneously with a mixed layer. The latter formed at the water-sediment interface on both sides of the scarp whenever a rupture occurred.

The diapirs of varve fragments (Figure 5) could have intruded into the mixed layers only before the layers consolidated, but they also postdate the shake that produced

the mixed layers. Aftershocks that hit the area before the consolidation of the mixed layers provide a plausible trigger to those diapirs.

Deformed layers of soft sediment somewhat similar to the mixed layers have been described around the world and identified as seismites [e.g., Davenport and Ringrose, 1987; Doig, 1991; Guiraud and Plaziat, 1993; Vittori et al., 1991], and references therein. The association of such soft sediment deformation with strong earthquakes is also backed by observations of recent events [Allen, 1986; Sims, 1975]. For example, resuspension of sediments was directly observed in lakes less than 10 km from the epicenter of the 1935 Témiskaming, Canada, M 6.3 earthquake. Piston cores recovered a 20-cm-thick chaotic layer, composed of tabular fragments of a previously formed silt layer [Doig, 1991]. What makes the mixed layers here special is their geometrical relationship to surface ruptures that formed them. Their widespread distribution beyond the fault zone offers an opportunity to study their occurrence pattern in columnar sections. Hence we suggest that each mixed layer formed during an earthquake just before the first undisturbed overlying lamina was deposited (Figure 7). The top of a mixed layer is the stratigraphic level at which the earthquake occurred. The time interval between earthquakes is represented by the distance between the tops of the mixed layers. The thickness of the mixed layers probably reflects the local intensity of the shaking (peak particle velocity, duration of motion, ground acceleration) as well as local sediment properties (composition, compaction, cohesion, particle size, and shape) and subtle lake bottom topography.
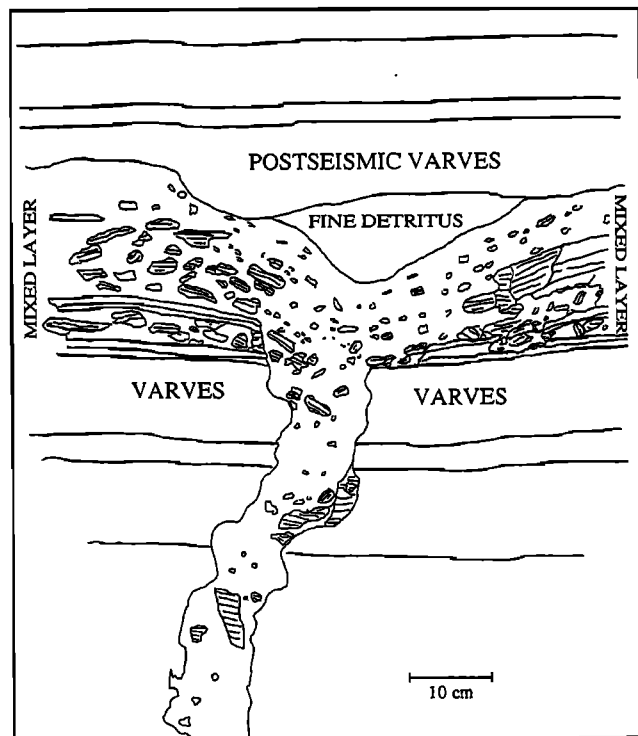
Figure 6. A fissure extends downward from a mixed layer. It is filled with the mixed material and is therefore contemporaneous. A lens of fine-grained detrital material fills a small depression at the top of the mixed layer. It is attributed to the compaction of the mixed material prior to the deposition of the overlying bed (traced from a photograph).
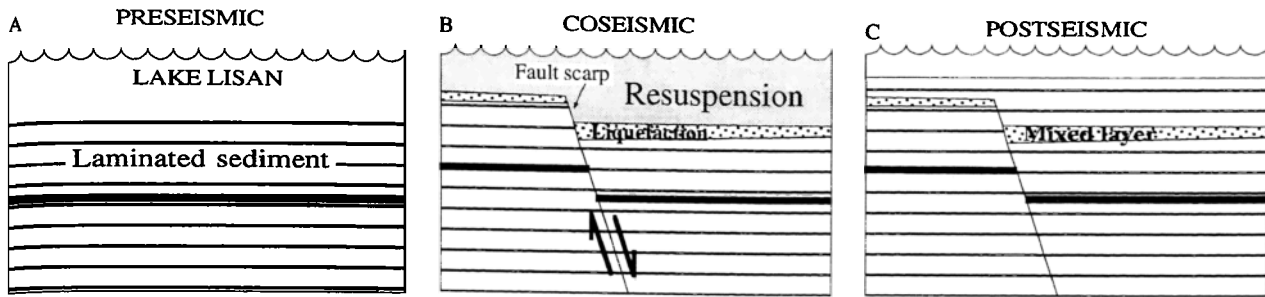
Figure 7. Interpretation of the fault-mixed layer association shown in Figure 3: (a) Laminated sediments are deposited at the bottom of Lake Lisan. (b) A fault ruptures the surface creating a subaqueous scarp. The coseismic movements deform, fluidize, and resuspend the sediment. A mixed layer forms on both sides of the fault scarp when the suspended sediments resettle. The mixed layer in the downthrown block is thicker. (c) Sedimentation continues; thicker sequence accumulates on the downthrown block. A second cycle of stages in Figures 7a-7c forms the configuration observed in Figure 4.

Previous studies in the Lisan Peninsula identified convolute folds as earthquake deformations [El-Isa and Mustafa, 1986; Seilacher, 1984], although no association with faults was reported. Our observations indicate that in places, folds are local slumps, limited by small-scale topography (e.g., Figure 4). Folded layers of alternating aragonite-detritus laminae are common throughout the Lisan Formation. At many localities the folded layers form half lenses (concave-bottomed), several millimeters to 1-1.5 m thick. In contrast to the widespread mixed layers, the folded layers extend over several centimeters to tens of meters. Their lower contacts are either flat or moderately arcuate décollement planes. The original thickness of the folded packages of varves varies between a few millimeters up to a few tens of centimeters; the thickest are 50-60 cm. The folds are commonly recumbent, asymmetric, or box-shaped. They recline in opposing directions, usually downdip. Previous studies [Karcz and Mimran, 1978; Mimran and Karcz, 1983] described the folds and revealed that in places the aragonite needles exhibit preferred orientation but very little breakage. We conclude that local slump structures were triggered either by the sediment self load or by weak seismicity which did not affect a large area. The formation of widespread mixed layers required significantly stronger shaking than that associated with the local slumps.

Provided that each mixed layer formed during an earthquake, we can now examine their temporal distribution.

Columnar Sections: Observations

In order to study the temporal distribution of earthquakes during Lisan time, we documented three detailed columnar sections of the Lisan Formation: PZ1 and PZ2 in the Peratzim Valley and M1 near Masada (Figure 1). The lowest age in section PZ1 (71 ka) is consistent with the base of the formation elsewhere [Kaufman et al., 1992]. In PZ2 the contact with the underlying formation is exposed, whereas in PZ1 it was found by digging 1 m. Near Masada (M1) the base is not exposed.

A total of 29 mixed layers were found along the 38.85 m of Section PZ1 and 34 layers in 41.32 m of Section PZ2, about 2 km apart. Twenty-eight mixed layers are found in 32.84 meters of section M1.

Section PZ2 is closer to the graben-bounding escarpment and contains several sand and conglomerate intercalations which do not reach section PZ1. Figure 8 shows an example of the correlation of lithologic units, in particular, mixed layers. The data available at present do not permit such a detailed correlation with the Masada outcrop. We are currently dating samples from the Masada section to enable the correlation with the Peratzim Valley sections. The correlation of individual mixed layers may be difficult because their continuity is affected by attenuation or amplification due to bedrock topography and composition. Salt diapirs that are common in the Dead Sea basin [Neev and Emery, 1967] possibly attenuate seismic wave propagation. This may obstruct the continuity of the mixed layers. An example of such effect has been reported in the Ionian Islands [Stiros, 1994]. The effect of topography of the bedrock below the soft sediments was demonstrated in the San Francisco 1906 earthquake, where burried vallies amplified ground movements and displacements [O'Rourke et al., 1992].

The locations of the mixed layers, their thicknesses, and the distance from each top to the previous one (the interval) are presented in Table 2. We assume that the earthquake record is complete, although it is possible that the formation of a thick mixed layer may have obliterated a former one or more. It also seems possible that two or more temporally close events are represented by a single mixed layer. The diapirs that intrude mixed layers (Figure 5) possibly record this scenario.

Discussion

Temporal Distribution

The mean intervals between the upper contacts of the mixed layers are 101 cm in section M1, 130 cm in PZ1, and 109 cm in section PZ2. The standard deviations are 100 cm in section M1, 199 cm in section PZ1, and 123 cm in PZ2. The coefficient of variation (the ratio of the standard deviation to the mean) is 1 in section M1, 1.53 in section PZ1, and 1.13 in section PZ2. The mean time interval between successive upper contacts in section PZ1 is 1.6 kyr with a standard deviation of 2.86 kyr, giving a ratio of 1.75 (Table 3). The ratio standard deviation/mean was suggested to quantify the degrees of periodicity or clustering in the temporal distribution [Ben-Zion and Rice, 1995; Kagan and Jackson, 1991]. The numerical simulations of Ben-Zion and Rice suggest that this ratio decreases with earthquake size and with the level of geometrical regularity of the fault system.

The ages determined in section PZ1 allow the transformation of thickness to temporal intervals by dividing
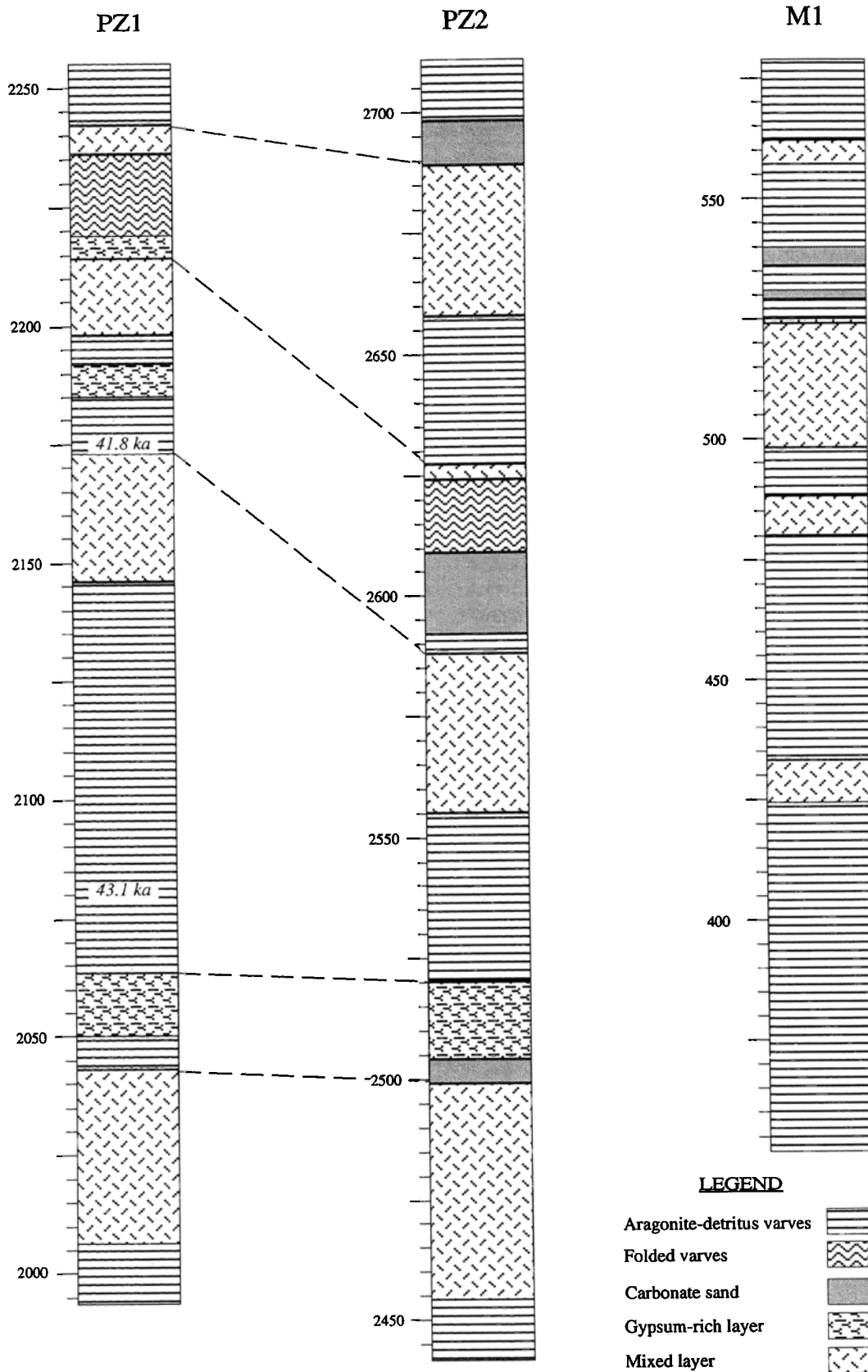
Figure 8. An example of segments of sections PZ1 and PZ2 in the Peratzim Valley and M1 near Masada. The level is measured in centimeters from the base of the Lisan Formation. Detailed correlation is hindered by facies variations. We suggest a tentative correlation between PZ1 and PZ2, which will be tested by radiometric dating.

Table 2. The locations of the Mixed Layers in Columnar Sections PZ1 and PZ2 in the Peratzim Valley and M1 near Masada (Figure 1)

Top cm	Age, ka	Bottom, cm	Thickness, cm	Interval, cm
		Section PZ1		
3862	24.4	3850	12	150
3712	26.1	3707	5	18
3694	26.3	3687	7	139
3555	27.8	3543	12	81
3474	28.6	3472	2	5
3469	28.7	3454	15	22
3447	28.9	3440	7	143
3304	30.5	3289	15	99
3205	31.6	3195	10	196
3009	33.7	2994	15	394
2615	38	2595	20	373
2242	42.1	2236	6	28
2214	42.4	2198	16	41
2173	42.8	2146	27	130
2043	44.2	2006	37	133
1910	45.7	1900	10	29
1881	46	1873	8	36
1845	46.4	1829	16	143
1702	48	1690	12	38
1664	48.4	1647	17	225
1439	50.8	1436	3	19
1420	51	1417	3	26
1394	51.3	1379	15	34
1360	51.7	1346	14	40
1320	52.1	1272	48	105
1215	55.4	1195	20	41
1174	55.7	1164	10	14
1160	55.7	1110	50	1026
134	71	125	9	34
Average			15	130
S.D.			12	199
		Section PZ2		
3701		3698	3	15
3686		3683	3	23
3663		3657	6	106
3557		3554	3	50
3507		3489	18	24
3483		3477	6	15
3468		3463	5	26
3442		3437	5	83
3359		3350	9	15
3344		3334	10	47
3297		3294	3	21
3276		3270	6	53
3223		3220	3	203
3020		3017	3	12
3008		3006	2	29
2979		2975	4	80
2899		2895	4	210
2689		2658	31	62
2627		2624	3	39
2588		2555	33	89
2499		2454	45	244
2255		2248	7	140
2115		2110	5	389
1726		1721	5	99
1627		1617	10	273
1354		1341	13	33
1321		1305	16	174
1147		1128	19	58
1089		1075	14	37
1052		1049	3	34

Table 2. (continued)

Top cm	Age, ka	Bottom, cm	Thickness, cm	Interval, cm
1018		1012	6	63
955		935	20	59
896		866	30	491
405		400	5	405
Average			11	109
S.D.			10	123
		Section M1		
2826		2824	2	89
2737		2736	1	94
2643		2641	2	46
2597		2595	2	44
2553		2549	4	45
2508		2505	3	164
2344		2342	2	45
2299		2296	3	47
2252		2250	2	49
2203		2200	3	55
2148		2145	3	162
1986		1984	2	59
1927		1925	2	48
1879		1878	1	457
1422		1417	5	140
1282		1274	8	72
1210		1207	3	100
1110		1108	2	193
917		915	2	365
552		547	5	38
514		488	26	36
478		470	8	55
423		414	9	143
280		275	5	93
187		185	2	38
149		147	2	13
136		118	18	20
116		111	5	116
Average			5	101
S.D.			5	100

The top and bottom of each layer are measured in centimeters from the base of the section. The interval is measured from the top of the mixed layer to the top of the former one below. Section PZ1 includes the absolute ages interpolated from the linear regression (Figure 3).

the intervals with the mean sedimentation rate. Sedimentation rates are calculated in two ways (Figure 3): by linear regression of all data and of three segments of the section. The age of the top of each mixed layer is then interpolated, and the time intervals are averaged. The mean recurrence interval in section PZ1 is about 1600 years, in agreement with other estimates for the last 4000 years [Ben-Menahem, 1991; Garfunkel et al., 1981; Reches and Hoexter, 1981]. Ages of sections PZ2 and M1 are not available yet; we tentatively assume similar sedimentation rates because of the similar stratigraphy. Most of the lithologic units of sections PZ1 and PZ2 correlate (Figure 8). The general division of the Lisan into lower detritus-rich and upper aragonite-rich units separated by a thin gypsum-rich unit is common to all three sections. We tentatively adopt Begin's [1974] correlation based on these units. Correlation with contemporaneous events recorded by

Table 3. Mean Interval Between the Upper Contacts of the Mixed Layers (M), Standard Deviation (S), and Ratio S/M

Section	Unit	M	S	S/M
PZ1 (three segments)	kyr	1.63	2.86	1.75
PZ1 (single regression)	kyr	1.49	2.26	1.51
PZ1	cm	130	199	1.53
PZ2	cm	109	123	1.13
M1	cm	101	100	0.99

The intervals are kiloyears in PZ1, where U series ages have been measured, and centimeters in all three sections. The mean sedimentation rate in PZ1 was calculated twice (Figure 3): by a single linear regression and by dividing the section into three segments. The mean intervals for both ways of calculations are presented.

Amit et al. [1994] in the southern Arava, some 180 km south of our study area, is not established.

Figure 9 displays the population of the time intervals between the mixed layers (the interseismic interval) illustrating the rarity of long intervals. This is also evident in Figure 10 that shows that the mixed layers in all three sections are clustered. The detailed stratigraphic correlation between the sections is not fully resolved because of slight facies changes (more ages are currently being measured in order to determine the precise correlation). However, the pattern of clustering is robust in all sections. In section PZ1 the earthquakes appear clustered during periods of 8-12 kyr, with relatively quiet periods of similar duration between the clusters (Figure 10). This pattern is independent of our choice of calculated sedimentation rate. Each cluster exhibits a different fine structure (i.e., the detailed distribution of events), limiting the predictability of the sequence. However, a period of the order of 20,000 years is likely to include a complete cycle of both a cluster and a quiet period. A mean recurrence time that is calculated for shorter periods may not represent the long-term seismic behavior.

Magnitudes

The assignment of magnitudes to the mixed layers can promote seismotectonic analysis because magnitudes, moments, fault area, and slip are all related [e.g., *Kanamori and Anderson*, 1975; *Wells and Coppersmith*, 1994].

Liquefaction is a major cause of damage during large earthquakes [*Youd and Perkins*, 1987]. Direct observations as well as experiments indicate that liquefaction related to earthquakes is mainly associated with those of magnitude 6 and more [*Allen*, 1982]. The dominant cause of liquefaction of loose, water-saturated, clastic sediments is cyclic loading by earthquake surface waves that subject the sediment to repeated horizontal shaking [*Allen*, 1982].

The thicknesses of the mixed layers in each columnar section obey a log-linear frequency distribution (Figure 11), similar to the behavior of earthquake magnitudes [*Gutenberg and Richter*, 1954]. Yet, it is wrong to assign magnitudes to mixed layers because in addition to magnitude, the thickness of a mixed layer is influenced also by subtle bottom topography (Figure 4) as well as variables such as peak particle velocity, duration of motion, ground acceleration, and local sediment properties. There is no correlation between the thickness of the mixed layers and the preceding interval (Figure 12). The large number of unknown variables, in addition to the weak correlation of acceleration with magnitude, hinders the assignment of earthquake magnitudes to the observed mixed layers. However, a general idea about magnitudes may be gained by comparison with observed liquefaction and fluidization elsewhere. The ground surface acceleration during earthquakes that are associated with liquefaction is of the order of 0.2g and the frequencies are mostly in the range 0.1-10 Hz [*Richter*, 1958]. For example, at a site undergoing liquefaction, simultaneous measurements of pore water pressure and ground accelerations during the Superstition Hills, California, M=6.6 earthquake reveal that excess pore pressures were generated once horizontal acceleration reached 0.21g. In other earthquakes, excess pore pressure did not occur at 0.17g [*Holzer et al.*, 1989].

Intensity VII of the Modified Mercalli Intensity Scale is the lowest that includes "water turbid with mud" [*Grünthal*, 1993]. This intensity occurs where the peak ground acceleration is 0.1g to 0.15g and the average peak velocity is 8-12 cm/s. In
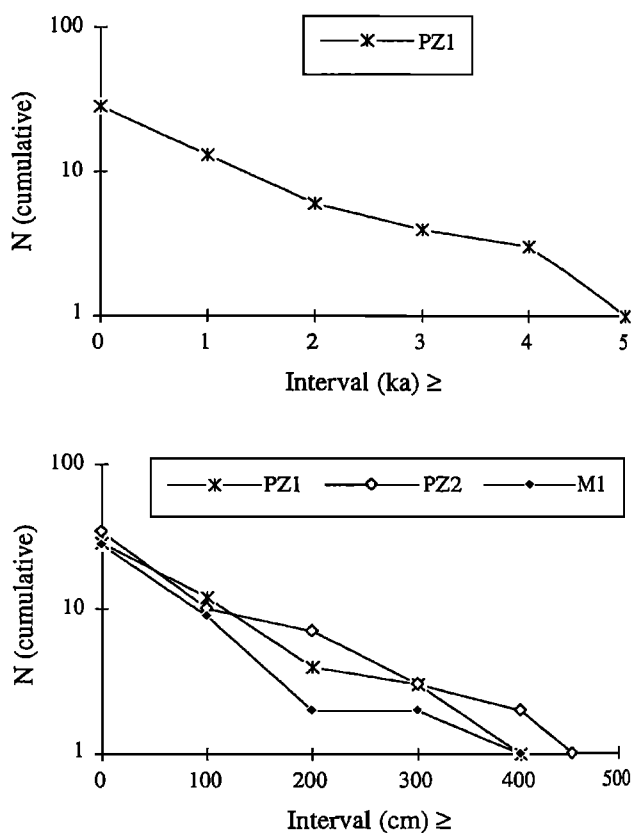
Figure 9. The frequency N of intervals is plotted as a function of their length. Long intervals are rare, and shorter intervals are progressively more common. N, shown on a log scale, is the number of individual intervals equal to or greater than the abscissa value. An interval is the vertical distance between upper contacts of two consecutive mixed layers in a columnar section. It can be transformed into a time interval by dividing by the sedimentation rate. (top) Population of time intervals in section PZ1 where ages have been determined and sedimentation rate is known. (bottom) Population of thickness intervals, exhibiting similar behavior in all three columnar sections.
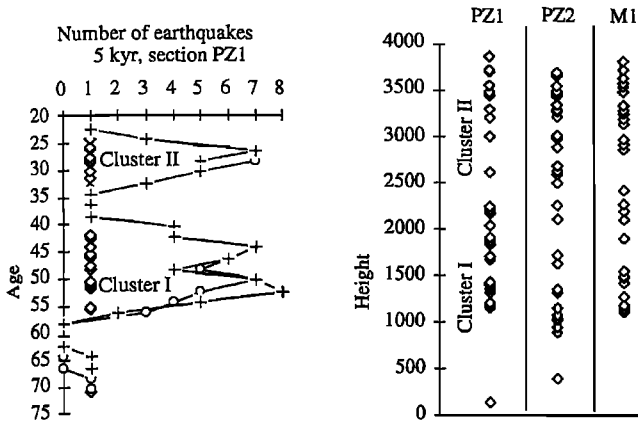
Figure 10. (left) The distribution of mixed layers (i.e., earthquakes) along section PZ1; open diamonds show the individual layers. Crosses and open circles are the number of earthquakes per 5 kyr sliding window, shifted by 2-kyr increments leaving 3-kyr overlap. The crosses show the distribution when the ages of the mixed layers are calculated by a single linear regression, whereas the circles show the distribution when the ages are calculated in three segments (Figure 3). The distribution shows two clusters of frequent events. A cycle about 20,000 years long includes a cluster period and a quiet intercluster period. The pattern of clustering is independent of our choice of calculated sedimentation rates. (right) The distribution of individual mixed layers along sections PZ1, PZ2, and M1. The top of the Lisan is used as a datum. All three sections show clusters of mixed layers separated by quiescent intervals.

Figure 12. No correlation is found between the thickness of a mixed layer and the thickness of undisturbed layers below it (deposited in the interseismic interval).

the 1906 San Francisco earthquake, intensity VII was reported on the San Francisco peninsula within 3 km to about 15 km from the San Andreas fault [*Bolt*, 1988]. In the Bingöl, Turkey, M_s=6.7 earthquake, intensity VII occurred up to 10 km from the fault [*Seymen and Aydin*, 1972]. Out of 58 observed sites that liquefied during earthquakes, 54 occurred during events of $M \geq 6$ and maximum accelerations of 0.08g-0.25g [*Kuribayashi and Tatsuoka*, 1975; *Youd*, 1977]. Liquefaction of sand may occur at M as low as 5 [*Audemard and de Santis*, 1991] and 4.6 [*Sims and Garvin*, 1995], but a quantitative analysis [*Allen*, 1986] based on observations [*Kuribayashi*
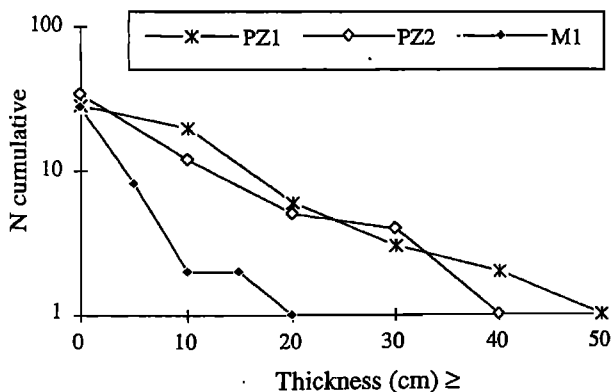

Figure 11. The frequency N of mixed layers is plotted as a function of their thicknesses. Thicker mixed layers are progressively rare, whereas thinner ones are more common. N, shown on a log scale, is the number of mixed layers whose thickness is equal to or greater than the abscissa value.
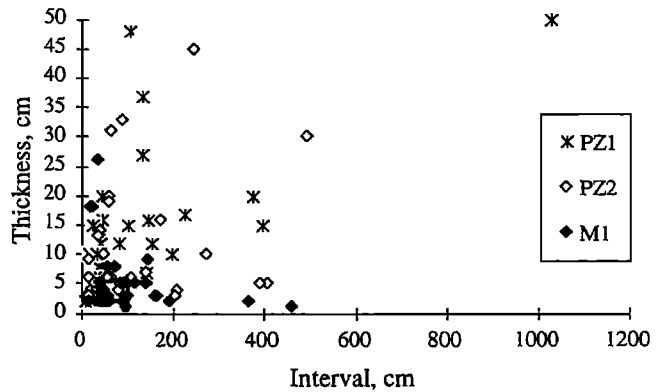
and *Tatsuoka*, 1975; *Youd*, 1977] indicates that it is more characteristic of greater magnitudes. The clay content in the Lisan (20-35%) and the grain sizes of a few microns [*Arkin and Michaeli*, 1986; *Begin et al.*, 1974] make it less prone to liquefaction than sand [*Allen*, 1982; *Seed et al.*, 1983]. For epicentral distances exceeding 100 km, M_s 7.5 appears to be a minimum threshold [*Vittori et al.*, 1991]. By comparison, it seems reasonable that the mixed layers of the Lisan Formation also formed during earthquakes with magnitudes 5.5-7 in the vicinity of the Dead Sea. We cannot constrain the maximum magnitude, and it is also possible that the mixed layers record magnitudes above 7 that occurred within distances of the order of 100 km and more. The distinction between weak and near earthquakes and far but strong ones seems, as yet, impossible. The character of the mixed layers indicates that their formation involved fluidization which requires stronger shaking than liquefaction [*Lowe*, 1975]. Magnitude 5.5 is therefore a conservative lower bound. The surface ruptures near Masada provide an independent constraint for the magnitude since surface faults are rarely reported below magnitude 5.5 [*Wells and Coppersmith*, 1994].

Finding the "missing link" between any measurable feature of the mixed layers and earthquake magnitudes will contribute to a better constraint on the long-term frequency-magnitude relation, maximum possible magnitude, and the seismic efficiency of the Dead Sea Transform. Such a link may be sought by correlating mixed layers in the post-Lisan sediments with historically or instrumentally recorded earthquakes.

Conclusions

The fine alternating aragonite and detritus laminae of the Lisan Formation provide highly sensitive markers that allow recognition of millimeter-scale deformation. Widespread layers composed of mixtures of brecciated laminae are identified as seismites, earthquake-induced deformations of the sediment. Assuming that each mixed layer is a seismite that formed in a single, $M_L \geq 5.5$ event, we conclude that the long-term mean recurrence period of strong ($M_L \geq 5.5$) earthquakes in the Dead Sea graben is about 1.6 kyr with a large standard deviation of about 2.8 kyr. The earthquakes cluster at periods of ~10,000 years separated by quieter periods of similar length. This clustering suggests that a mean recurrence time

determined for less than 20,000 years might misrepresent the long-term behavior of the fault zone.

References

Agnon, A., The evolution of sedimentary basins and the morphotectonics in the western fault escarpment of the Dead Sea (in Hebrew, English abstract), M.Sc. thesis, Hebrew Univ., Jerusalem, 1983.

Allen, C. R., Seismological and paleoseismological techniques of research in active tectonics, in *Active Tectonics*, edited by R. E. Wallace, 148-154, National Academy Press, Washington, D.C., 1986.

Allen, J. R. L., *Sedimentary Structures: Their Character and Physical Basis*, 663 pp., Elsevier, New York, 1982.

Allen, J. R. L., Earthquake magnitude-frequency, epicentral distance, and soft-sediment deformation in sedimentary basins, *Sediment. Geol.*, 46, 67-75, 1986.

Amit, R., J. B. J. Harrison, Y. Enzel, and N. Porat, Paleoseismology in the southern Arava rift, Israel, *U.S. Geol. Surv. Open File Rep.*, 94-568, 8-10, 1994.

Arieh, E. J., Seismicity of Israel and adjacent areas, *Isr. Geol. Surv. Bull.*, 43, 1-14, 1967.

Arkin, Y., and L. Michaeli, The significance of shear strength in the deformation of laminated sediments in the Dead Sea area, *Isr. J. Earth Sci.*, 35, 61-72, 1986.

Audemard, F. A., and F. de Santis, Survey of liquefaction structures induced by recent moderate earthquakes, *Bull. Int. Assoc. Eng. Geol.*, 44, 5-16, 1991.

Begin, Z. B., A. Ehrlich, and Y. Nathan, Lake Lisan, the Pleistocene precursor of the Dead Sea, *Geol. Surv. Isr. Bull.*, 63, 30, 1974.

Ben-Menahem, A., Four thousand years of seismicity along the Dead Sea rift, *J. Geophys. Res.*, 96, 20,195-20,216, 1991.

Ben-Menahem, A., A. Nur, and M. Vered, Tectonics, seismicity and structure of the Afro-Eurasian junction- the breaking of an incoherent plate, *Phys. Earth Planet. Inter. 12*, 1-50, 1976.

Ben-Zion, Y., and J. R. Rice, Slip patterns and earthquake populations along different classes of faults in elastic solids, *J. Geophys. Res.*, 100, 12,959-12,983, 1995.

Bentor, Y. K., and A. Vroman, The geological map of Israel, 1:100,000, Sheet 16, Mt. Sedom, Geol. Surv. of Israel, Jerusalem, 117, 1960.

Bolt, B. A., *Earthquakes*, 282 pp., W. H. Freeman, New York, 1988.

Chen, J. H., R. L. Edwards, and G. J. Wasserburg, ^{238}U, ^{234}U, and ^{232}Th in seawater, *Earth Planet. Sci. Lett.*, 80, 241-251, 1986.

Copeland, L., and C. Vita-Finzi, Archaeological dating of geological deposits in Jordan, *Levant, X*, 10-25, 1978.

Davenport, C. A., and P. S. Ringrose, Deformation of Scottish Quaternary sediment sequence by strong earthquake motions, in *Deformation of Sediments and Sedimentary Rocks*, edited by M. E. Jones and R. M. Preston, *Geol. Soc. Spec. Publ. London*, 29, 299-314, 1987.

Doig, R., Effects of strong seismic shaking in lake sediments, and earthquake recurrence interval, Témiscaming, Quebec, *Can. J. Earth Sci.*, 28, 1349-1352, 1991.

Edwards, R. L., J. H. Chen, and G. J. Wasserburg, ^{238}U-^{234}U-^{230}Th-^{232}Th systematics and the precise measurement of time over the past 500,000 years, *Earth Planet. Sci. Lett.*, 81, 175-192, 1987.

El-Isa, Z. H., and H. Mustafa, Earthquake deformations in the Lisan deposits and seismotectonic implications, *Geophys. J. R. Astron. Soc.*, 86, 413-424, 1986.

Enzel, Y., R. Amit, J. Bruce, J. Harrison, and N. Porat, Morphologic dating of fault scarps and terrace risers in the southern Arava, Israel: Comparison to other age-dating techniques and implications for paleoseismicity, *Isr. J. Earth Sci.*, 43, 91-103, 1994.

Field, M. E., J. V. Gardner, A. E. Jennings, and B. D. Edwards, Earthquake-induced sediment failure on a 0.25° slope, Klamath River delta, California, *Geology, 10*, 542-546, 1982.

Gardosh, M., Z. Reches, and Z. Garfunkel, Holocene tectonic deformation along the western margins of the Dead Sea, *Tectonophysics, 180*, 123-137, 1990.

Garfunkel, Z., I. Zak, and R. Freund, Active faulting along the Dead Sea transform (rift), *Tectonophysics, 80*, 1-26, 1981.

Grant, L. B., and K. Sieh, Paleoseismic evidence of clustered earthquakes on the San Andreas fault in the Carrizo Plain, California, *J. Geophys. Res.*, 99, 6819-6841, 1994.

Grünthal, G., *European Macroseismic Scale 1992*, 79 pp., Centr. Eur. de Geodyn. et de Seismol., Luxembourg, 1993.

Guiraud, M., and J. C. Plaziat, Seismites in the fluviatile Bima sandstone: identification of paleoseisms and discussion of their magnitudes in a cretaceous synsedimentary strike-slip basin (Upper Benue, Nigeria), *Tectonophysics, 225*, 493-522, 1993.

Gutenberg, B., and C. F. Richter, *Seismicity of the Earth and Associated Phenomena*, 310 pp., Princeton Univ. Press, Princeton, N. J., 1954.

Holzer, T. L., T. L. Youd, and T. C. Hanks, Dynamics of liquefaction during the 1987 Superstition Hills, California, earthquake, *Science, 244*, 56-59, 1989.

Hsü, K. J., *Physical Principles of Sedimentology*, 233 pp., Springer-Verlag, New York, 1989.

Kagan, Y. Y., and D. D. Jackson, Long-term earthquake clustering, *Geophys. J. Int.*, 104, 117-133, 1991.

Kanamori, H., and D. L. Anderson, Theoretical basis of some empirical relations in seismology, *Bull. Seismol. Soc. Am.*, 65, 1073-1095, 1975.

Karcz, I., and Y. Mimran, Soft sediment deformation in calcareous marls of Lisan Formation, in *Tenth International Congress on Sedimentol.*, Int. Assoc. of Sedimentol., Jerusalem, 349-350, 1978.

Katz, A., and N. Kolodny, Hypersaline brine diagenesis and evolution in the Dead Sea Lake Lisan system (Israel), *Geochim. Cosmochim. Acta, 53*, 59-67, 1989.

Katz, A., Y. Kolodny, and A. Nissenbaum, The geochemical evolution of the Pleistocene Lake Lisan-Dead Sea system, *Geochim. Cosmochim. Acta, 41*, 1609-1626, 1977.

Kaufman, A., U series dating of Dead Sea basin carbonates, *Geochim. Cosmochim. Acta, 35*, 1269-1281, 1971.

Kaufman, A., Y. Yechieli, and M. Gardosh, Reevaluation of the lake-sediment chronology in the Dead Sea Basin, Israel, based on new ^{230}Th/^{234}U dates, *Quat. Res.*, 38, 292-304, 1992.

Keefer, D. K., Landslides caused by earthquakes, *Geol. Soc. Am. Bull.*, 95, 406-421, 1984.

Kuribayashi, E., and F. Tatsuoka, Brief review of liquefaction during earthquakes in Japan, *Soils Found.*, 15, 81-92, 1975.

Lovell, J., S. Crampin, R. Evans, and S. Balamir-Ucer, Microearthquakes in the TDP swarms, Turkey: Clustering in space and time, *Geophys. J. R. Astron. Soc.*, 91, 313-330, 1987.

Lowe, D. R., Water escape structures in coarse-grained sediments, *Sedimentology, 23*, 285-308, 1975.

Marco, S., and A. Agnon, Prehistoric earthquake deformations near Masada, Dead Sea graben, *Geology, 23*, 695-698, 1995.

Marco, S., A. Agnon, M. Stein, and H. Ron, A 50,000 year continuous record of earthquakes and surface ruptures in the Lisan Formation, the Dead Sea graben, *U.S. Geol. Surv. Open File Rep.*, 94-568, 112-114, 1994.

Mimran, Y., and I. Karcz, Study of fabrics in sedimentary folds of Lisan Formation, in *Israel Geological Society Annual Meeting*, p. 55, Isr. Geol. Soc., Jerusalem, Nazaret, 1983.

Neev, D., and K. O. Emery, The Dead Sea, depositional processes and environments of evaporites, *Geol. Surv. Isr. Bull.*, 41, 147 pp., 1967.

Niemi, T. M., and Z. Ben-Avraham, Evidence for Jericho earthquakes from slumped sediments of the Jordan River delta in the Dead Sea, *Geology, 22*, 395-398, 1994.

O'Rourke, T. D., P. A. Beaujon, and C. R. Scawthorn, Large ground deformations and their effects on lifeline facilities: 1906 San Francisco earthquake, in *Case Studies of Liquefaction and Lifeline Performance During Past Earthquakes*, edited by T. D. O'Rourke and M. Hamada, 1-130, Natl. Cent. for Earthquake Eng. Res., Buffalo, N. Y., 1992.

Reches, Z., and D. F. Hoexter, Holocene seismic and tectonic activity in the Dead Sea area, *Tectonophysics, 80*, 235-254, 1981.

Richter, C. F., *Elementary Seismology*, 768 pp., W. H. Freeman, New York, 1958.

Salamon, A., Seismotectonic analysis of earthquakes in Israel and

adjacent areas (in Hebrew with English abstract), Ph.D. thesis, Hebrew Univ., Jerusalem, 1993.

Scholz, C. H., *The Mechanics of Earthquakes and Faulting*, 439 pp., Cambridge Univ. Press, New York, 1990.

Schramm, A., M. Stein, and S. L. Goldstein, Constancy of $^{234}U/^{238}U$ ratios in Late Pleistocene aragonitic sediments—Lake Lisan, paleo-Dead Sea, *Terra Nova*, 7, 325, Eur. Union. Geol. Meet. Suppl., 1995.

Seed, H. B., I. M. Idriss, and I. Arrango, Evaluation of liquefaction potential using field performance data, *J. Geotech. Eng., Am. Soc. Civ. Eng.*, 109, 458-482, 1983.

Segall, P., and D. D. Pollard, Mechanics of discontiuous faults, *J. Geophys. Res.*, 85, 4337-4350, 1980.

Seilacher, A., Fault-graded beds interpreted as seismites, *Sedimentology*, 13, 155-159, 1969.

Seilacher, A., Sedimentary structures tentatively attributed to seismic events, *Mar. Geol.*, 55, 1-12, 1984.

Seymen, I., and A. Aydin, The Bingöl earthquake fault and its relation to the North Anatolian fault zone, *Bull. Miner. Res. Explor. Inst. Turkey*, 79, 1-8, 1972.

Shapira, A., R. Avni, and A. Nur, A new estimate for the epicenter of the Jericho earthquake of 11 July 1927, *Isr. J. Earth Sci.*, 42, 93-96, 1992.

Shapira, A., and L. Feldman, Microseismicity of three locations along the Jordan rift, *Tectonophysics*, 141, 89-94, 1987.

Sims, J. D., Determining earthquake recurrence intervals from deformational structures in young lacustrine sediments, *Tectonophysics*, 29, 144-152, 1975.

Sims, J. D., and C. D. Garvin, Recurrent liquefaction induced by the 1989 Loma Prieta earthquake and 1990 and 1991 aftershocks: Implications for paleoseismicity studies, *Bull. Seismol. Soc. Am.*, 85, 51-65, 1995.

Stein, M., S. L. Goldstein, H. Ron, and S. Marco, Precise TIMS ^{230}Th - ^{234}U ages and magnetostratigraphy of Lake Lisan sediments (paleo Dead Sea), *Eos Trans. AGU*, 73(14), Spring Meet. Suppl., 154, 1992.

Stein, M., G. J. Wasserburg, P. Aharon, J. H. Chen, Z. R. Zhu, A. Bloom, and J. Chappell, TIMS U-series dating and stable isotopes of the last interglacial event in Papua New Guinea, *Geochim. Cosmochim. Acta*, 57, 2541-2554, 1993.

Stiros, S., Anomalous attenuation of seismic waves in the Ionian Islands, Greece, *Eos Trans. AGU*, 75, 117-118, 1994.

Swan, F. H., Temporal clustering of paleoseismic events on the Oued Fodda fault, Algeria, *Geology*, 16, 1092-1095, 1988.

van Eck, T., and A. Hofstetter, Fault geometry and spatial clustering of microearthquakes along the Dead Sea-Jordan rift fault zone, *Tectonophysics*, 180, 15-27, 1990.

Vita-Finzi, C., Observations on the Late Quaternary of Jordan, *Palestine Explor. Q., Jan.-June*, 19-33, 1964.

Vittori, E., S. S. Labini, and L. Serva, Palaeoseismology: Review of the state-of-the-art, *Tectonophysics*, 193, 9-32, 1991.

Wells, D. L., and K. J. Coppersmith, New empirical relationships among magnitudes, rupture length, rupture width, rupture area, and surface displacement, *Bull. Seismol. Soc. Am.*, 84, 974-1002, 1994.

Youd, T. L., Discussion of "Brief review of liquefaction during earthquakes in Japan" by E. Kuribayashi and T. Tatsuoka, *Soils Found.*, 17, 82-85, 1977.

Youd, T. L., and D. M. Perkins, Mapping of liquefaction severity index, *J. Geotech. Eng. Am. Soc. Civ. Eng.*, 113, 1374-1392, 1987.

A. Agnon, S. Marco, and M. Stein, Institute of Earth Sciences, Hebrew University, Jerusalem 91904, Israel. (e-mail: smarco@shum.cc.huji.ac.il)

H. Ron, Institute for Petroleum Research and Geophysics, P.O.Box 2286, Holon 58122, Israel.